energies

Article

Design and Evaluation of a Surfactant–Mixed Metal Hydroxide-Based Drilling Fluid for Maintaining Wellbore Stability in Coal Measure Strata

Shuya Chen, Yanping Shi, Xianyu Yang, Kunzhi Xie and Jihua Cai *

Faculty of Engineering, China University of Geosciences, Wuhan 430074, China; chenshuya@cug.edu.cn (S.C.); yunus@cug.edu.cn (Y.S.); yxy@cug.edu.cn (X.Y.); kunzhixie@gmail.com (K.X.)

* Correspondence: caijh@cug.edu.cn; Tel.: +86-27-6788-3507

Received: 27 February 2019; Accepted: 13 May 2019; Published: 16 May 2019

Abstract: Co-exploitation of coal measure gases (coalbed gas, shale gas, and tight sandstone gas) puts a higher requirement on drilling fluids. Conventional drilling fluids have disadvantages, such as causing problems of borehole collapse, formation damage, and water blockage. This paper proposes a set of high inhibitive and low-damage drilling fluids that function by electrical inhibition and neutral wetting. Zeta potential results showed that the negative electrical property of Longtan coal in Bijie, Guizhou, can be reversed by organic mixed metal hydroxide (MMH) and the cationic surfactant alkyl trimethylammonium bromide (CS-5) from −3.63 mV to 19.75 mV and 47.25 mV, respectively. Based on the contact angle and Fourier Transform Infrared Spectroscopy (FT-IR) results, it can be concluded that chemical adsorption dominates between the Longmaxi shale and surfactants, and physical adsorption between the Longtan coal and surfactants. A compound surfactant formula (0.001 wt% CS-4 + 0.001 wt% CS-1 + 0.001 wt% CS-3), which could balance the wettability of the Longmaxi shale and the Longtan coal, making them both appear weakly hydrophilic simultaneously, was optimized. After being treated by the compound surfactants, the contact angles of the Longmaxi shale and the Longtan coal were 89° and 86°, respectively. Pressure transmission tests showed that the optimized combination of compound surfactants and inorganic MMH (MMH-1) could effectively reduce permeability of the Longmaxi shale and the Longtan coal, thus retarding pore pressure transmission in coal measure strata. Then, the proposed water-based drilling fluid (WBDF) system (4 wt% sodium bentonite + 1.5 wt% sodium carboxymethyl cellulose + 2 wt% lignite resin + 5 wt% potassium chloride + 3 wt%MMH-1 + 0.001 wt% CS-4 + 0.001 wt% CS-1 + 0.001 wt% CS-3) was evaluated based on parameters including rheology, American Petroleum Institute (API) filtration, electrical property, wettability, inhibition capability, reservoir protection characteristics, and anti-pollution performance. It had an API filtration of 7 mL, reservoir damage rate of 10%, moderate and acceptable viscosity, strong inhibition capability to coal measure strata rocks, good tolerance to inorganic pollutants and drilling cuttings, and environmentally friendly properties. It could meet wellbore stability and reservoir protection requirements in the co-exploitation of coal measure gases.

Keywords: coal measure gases (coalbed gas; shale gas; and tight sand gas); co-exploitation; wellbore stability; wettability; zeta potential; drilling fluid

1. Introduction

Coal measure gases (CMG), including coalbed methane (CBM), tight sandstone gas, and shale gas, are important unconventional gas resources. Recent exploration results have revealed the presence of shale gas and tight sandstone gas in the Qinshui basin, located in Shanxi, China, which is an important area of CBM production [1]. Furthermore, in the upper Permian coal bearing strata of the Liupanshui coalfield, the overlaid coal seam and shale have reached the level of high-quality source rock [2]. However, single-reservoir exploitation is always accompanied with problems, such as low production, short drainage periods, and high cost [3]. In order to improve the productivity and utilization efficiency of unconventional gas resources, co-exploitation of CMG is a key factor in the development system [4]. Drilling fluid, known as the blood of drilling engineering, is a vital technique [5]. Besides for balancing formation pressure, cooling and lubricating drilling tools, and carrying drilling cuttings, the main functions of coal measure strata drilling fluid are to maintain wellbore stability and minimize formation damage [6].

Large amounts of natural cleats and tectonic fractures and water-sensitive clay minerals cause borehole collapse and formation damage problems in CMG reservoirs [7,8]. Clay swelling and the water blockage of drilling fluid invasion can reduce the permeability in the near wellbore regions, leading to low productivity of CMG wells [9,10]. Conventional drilling fluids, such as potassium chloride drilling fluid and low solid-phase polymer drilling fluid, may cause leakage problems and borehole collapse due to their low density [11]. In this case, a set of formation-compatible drilling fluids need to be proposed. Several studies were carried out using nanoparticles (NPs) to improve wellbore stability by plugging pore throats, reducing the reservoir permeability and building a thin, tight mud cake [12]. Several types of nanoparticles were investigated, such as cellulose nanocrystals [13], multi-walled carbon nanotubes [14], and different clay particles [15,16]. Accordingly, some researchers proposed rheological models of nanoparticle-based drilling fluid to better estimate the shear stress and viscosity under downhole conditions [17,18]. However, the stability of nanoparticle dispersions remains a huge challenge, along with the agglomerate problem and the high cost, and therefore NP-drilling fluid applications in the industry have not been fully implemented.

Wettability is one of the most important surface properties of rock [19]. It controls the magnitude and direction of capillary force and affects fines migration [20,21]. The wettability of a solid surface can be quantified by contact angle θ via Yang's equation [22]. Generally, when the contact angle is smaller than 90°, the solid surface is considered to be water-wet. If the contact angle is larger than 90°, the solid surface is considered to be oil-wet [23]. Given the pore throat distribution of shale/coal, the invasion of water/filtrate will form a meniscus pointing to the water/filtrate, after which the capillary force is formed [24]. According to the capillary force formula proposed by Liang et al. [25], when the contact angle is equal to 90° (neutral wetting), the capillary force is minimum, which is beneficial to borehole stability and reservoir protection.

Surfactants have been wildly used in production engineering to promote oil recovery rates by changing capillary forces and altering reservoir wettability [26]. They have also been used as emulsifiers in oil-based drilling fluid and as shale-swelling inhibitors to prevent wellbore instability [27]. However, there are not many reports about the application of surfactants in water-based drilling fluid. Yunita et al. [28] discovered that the rheological and filtration properties of water-based drilling fluid were improved with the addition of nonionic and anionic surfactants. Shadizadeh et al. [29] developed a plant-based nonionic surfactant zizyphus spina-christi extract (ZSCE), which showed excellent inhibitive ability to shale. The ZSCE molecules could form a hydrophobic shell on the clay surface through hydrogen bonding between the hydrophilic tail of ZSCE and oxygen atoms available on the silica surface of clay. Our previous study proposed a set of compound surfactants that could increase the contact angle of shale from 34.28° to 64.54° and improve the inhibition of water-based drilling fluid [30]. Compared to the old surfactant formula, this research proposed a set of cationic compound surfactants. After treatment with the proposed surfactants, the contact angles of the Longmaxi shale and the Longtan coal were 89° and 86°, respectively.

Due to the cation exchange capacity of clay minerals, an electrical-double-layer (EDL) can be formed in water systems. Zeta potential (ζ, mV), known as the potential between the slipping plane and the bulk solution, has traditionally been used to measure the stability of clay dispersions and estimate the double-layer thickness [31,32]. The nature of the EDL controls the repulsion/attraction of the system [33]. If the clay zeta potential is smaller than −60 mV, the system is extremely dispersive, if the zeta potential is around −40 mV, the system is strongly dispersive, if the zeta potential is around −20 mV, the system is probably dispersive, and if the zeta potential is close to zero, the system is non-dispersive [34]. Zhang et al. [35] found that the water adsorption rate of clay minerals showed a good correlation with zeta potential, and the negative charge of the formation was the dominant reason of swelling. Therefore, it is feasible to improve drilling fluid inhibition by increasing its zeta potential.

In addition to indicating colloid stability and clay swelling, zeta potential plays a significant role in understanding the adsorption mechanism of inorganic/organic molecules at the solid/solution interface [32]. Previous studies showed that the electric double layer is closely related to wettability [36,37]. Zeta potential measurements can be used to evaluate the stability of the water membrane on a rock surface. If the membrane is instable (zeta potential is between −30 mV and +30 mV), the rock surface is considered to be neutral wetting or oil-wet [38]. Arif et al. [39] measured zeta potentials as a function of temperature and salinity for different ranks of coals. Results showed that zeta potential increased with salinity and coal rank, and contact angle also increased with salinity and coal rank, implying a positive relation between zeta potential and wettability. Song et al. [40] pointed out that coal surfaces appeared to be hydrophobic when zeta potential was close to zero.

Su et al. [34] proposed organic mixed metal hydroxide (MMH) treatment, electrolyte treatment and pH adjustment to control the electrical properties of clay minerals and drilling fluid. Li et al. [41] tested the zeta potential of coal as a function of pH. Results showed that coal particles were negatively charged when the solution was strongly acidic, and then the zeta potential increased when solution became alkaline. Shu et al. [42] developed a modified low-damage mixed metal hydroxide (MMH) drilling fluid system for carbonate reservoirs. Not only can the MMH form a special spatial network structure with bentonite, it can be easily removed by oil or acid, which can further improve/recover reservoir permeability. Furthermore, the structure of MMH–bentonite is larger than the formation pore throat, which limits the invasion depth of the drilling fluid.

Based on previous studies, a set of low-damage, high-inhibitive, water-based drilling fluids based on wettability alteration and electrical inhibition, which could meet wellbore stability and formation protection requirements in the co-exploitation of CMG, was proposed. This paper developed a set of compound surfactant formulas that could effectively reduce the hydrophilicity of the reservoir surface along with the optimized MMH additive, which showed great ability to avoid clay hydration by electrical inhibition. Furthermore, the pressure transmission results confirmed their potential to increase wellbore stability in coal measure strata Among the numerous drilling fluid systems, this paper paves a new way for the design of coal measure strata drilling fluids

2. Materials and Methods

2.1. Materials

The surfactants used in this study were sodium alkylbenzene sulfonate (AS-1), sodium dodecyl sulfate (AS-2), alkyl trimethylammonium chloride (CS-1), alkyl trimethylammonium bromide (CS-2), double-chain quaternary ammonium surfactant (CS-3), benzylmethyl ammonium chloride (CS-4), and alkyl three methyl ammonium bromide (CS-5). Organic MMH (MMH-2) is a light yellow transparent liquid and is easily soluble in water and oil. Inorganic MMH (MMH-1) is a white powder and is soluble in water.

Among drilling fluid additives used, the bentonite used was sodium bentonite, which is widely used in the industry. Sodium carboxymethyl cellulose is a white particulate powder and is soluble in water. Lignite resin is a black powder and is stable at high temperature. Potassium chloride is a white crystalline small particle powder with a purity greater than 99.5%.

Sandstone is barely sensitive to water, and there is almost no appearance of wellbore instability in sandstone formation. This research focused on shale and coal formations, which are troublesome formations in coal measure strata. Shale samples used were collected from the Lower Silurian Longmaxi group, Xiushan, Southwest China (the Longmaxi shale). Coal rock samples used were taken from the

Longtan group, Bijie, Southwest China (the Longtan coal). Tables 1 and 2 present mineral compositions of the Longmaxi shale and the Longtan coal using the X-ray diffraction (XRD) method.

Table 1. Mineral composition of the Longmaxi shale samples.

Minerals	Chlorite	Illite	Calcite	Feldspar	Quartz	Dolomite
Contents (%)	10	10	25	5	47	3

Table 2. Mineral composition of the Longtan coal samples.

Mineral Name	Illite	Kaolinite	Albite	Pyrite	Amorphous
Contents (%)	22	7	4.9	1.1	65

2.2. *Methodology*

2.2.1. X-ray Diffraction (XRD)

Mineral compositions of the Chongqing Longmaxi shale and the Guizhou Longtan coal samples were obtained by an X' Pert PRO Diffractometer (Panalytical B. V., Almelo, The Netherlands). The XRD test was conducted by the State Key Laboratory of Geological Process and Mineral Resources. The quantitative analyses of the samples were performed by XrayRun software. As for the Longtan coal samples, 1 wt% of high-purity silicon (>99.99%) was added into the coal samples as an internal standard. The crystalline minerals were determined using XrayRun, the remains were amorphous mineral (organic matter and minerals with low crystallinity) content. Results are shown in Tables 1 and 2.

Shale is a sedimentary rock and often consists of quartz, clays, and other silicate and carbonate minerals. It usually has low porosity of 2 to 4% [43], and it has very low permeability of 5–100 × 10^{-5} mD and a compressive strength of 250–300 MPa [44]. Due to its high clay concentration, it tends to swell in water or drilling fluids, causing instability problems of the wellbore. The Longmaxi shale (outcrops) was located in Xiushan County, south of Chongqing City, southwest China. As shown in Table 1, the Longmaxi shale consisted of 47 wt% quartz, 25 wt% calcite, and 20 wt% clay minerals (10 wt% chlorite and 10 wt% illite), which means the Longmaxi shale samples have moderate water sensitivity and brittleness.

The Longtan coal samples were collected from the PQT-1 well, Pu'an county, southwest of Guizhou Province, southwest China. The Longtan coal was black and had weak metallic gloss. Cracks were developed, and with such a clear layered structure, the samples were easily broken. According to Table 2, the Longtan coal had 29.05 wt% clay minerals (22.05 wt% illite and 7 wt% kaolinite), indicating the Longtan coal rock had medium water-sensitivity.

2.2.2. Fourier Transform Infrared Spectroscopy (FT-IR)

The FT-IR spectra of the Longmaxi shale and Longtan coal samples were measured by a Bruker Vertex 70 FTIR spectrophotometer (Bruker Technology Co., Ltd., Madison, WI, USA). Each 2 mg sample was fully mixed with 200 mg potassium bromide pellets. Its resolution was 1.6 cm^{-1} and the measured region extended from 4000 to 400 cm^{-1}.

2.2.3. Zeta Potential Test

Zeta potential of the Longtan coal surface was investigated by a Zetasizer Nano ZS90 nanoparticle size and zeta potential analyzer (Malvern Instruments Ltd., Malvern, UK). Coal powders passing through a 120-mesh sieve were poured into testing liquids. After ultrasonic oscillation treatment for 10 min, the supernatants were removed to check their zeta potentials.

2.2.4. Contact Angle and Surface Tension

Wettability can be used to describe the interaction between oil, water, and reservoir rocks, which can be characterized by the contact angle ($\theta°$). Contact angles of the Longmaxi shale and the Longtan coal samples were measured by a JC2000C contact angle measuring instrument (Shanghai Zhongchen Digital Technology Equipment Co., Ltd., Shanghai, China). Polished Longtan coal and Longmaxi shale samples were soaked in different surfactant solutions for 24 h, then flushed with water for 10 s to remove residual surfactant, then dried under 100 °C for 2 h and cooled under ambient temperature. Finally, a water droplet was dropped on the polished side of core samples, and photos were recorded by a computer connected to the JC2000C contact angle measuring instrument. The contact angle measurement was conducted using contact angle test software with the angle measuring method. Surface tension of different solutions was tested by a QBZY-2 automatic surface tension meter (Shanghai Fangrui Instrument Co., Ltd., Shanghai, China). Each test was repeated three times to check the confidence of the test.

2.2.5. Pressure Transmission Test

The capability of various fluids to retard pore fluid pressure transmission into rock samples in contact with varied fluids was evaluated with an HKY-3 pressure transmission device developed by Hai'an Petroleum Scientific Research Instrument Co., Ltd., Nantong, China. The basic principle of the pressure transmission test (PTT) is to establish pressure difference on the upper and lower side of the core samples, and the equipment can detect the dynamic change of closed fluid at the upper and the lower end, through a pressure transducer, under the conditions of steady upstream pressure. The experimental setup of the HKY-3 pressure transmission device is shown in Figure 1. Data (including confining pressure, upstream pressure, and downstream pressure) were monitored and recorded by the computer every 60 s. The confining pressure and upstream pressure for the Longmaxi shale and the Longtan coal were 5.5 MPa and 4.5 MPa, and 3 MPa and 2 MPa, respectively. Furthermore, the permeability of the tested core samples was calculated by Equation (1):

$$\mathrm{k} = \frac{\mu\beta VL}{A}\frac{\Delta\ln\left[(P_m - P_0)/\left(P_m - P_{(1,t)}\right)\right]}{\Delta t} \tag{1}$$

where k is permeability of the core sample in μm^2, μ is viscosity of downstream reservoir fluid in cP, β is fluid static compression ratio in 10 MPa^{-1}, V is downstream confined volume in cm^3, L is core length in cm, A is core cross section area in cm^2, P_m is upstream pressure in MPa, P_0 is core pore pressure in MPa, $P_{(1,t)}$ is T-time downstream pressure in MPa, Δt is time difference in s.

The core samples used in this study were drilled from rock outcrop collected from the field. The drilled core samples were then cut into slices using a core cutter, flushed with water for 30 s to avoid contaminations, and then dried at 105 °C for 24 h. The Longmaxi shale samples were 5 mm thick and 25 mm in diameter, and the Longtan coal samples were 10 mm thick and 25 mm in diameter.

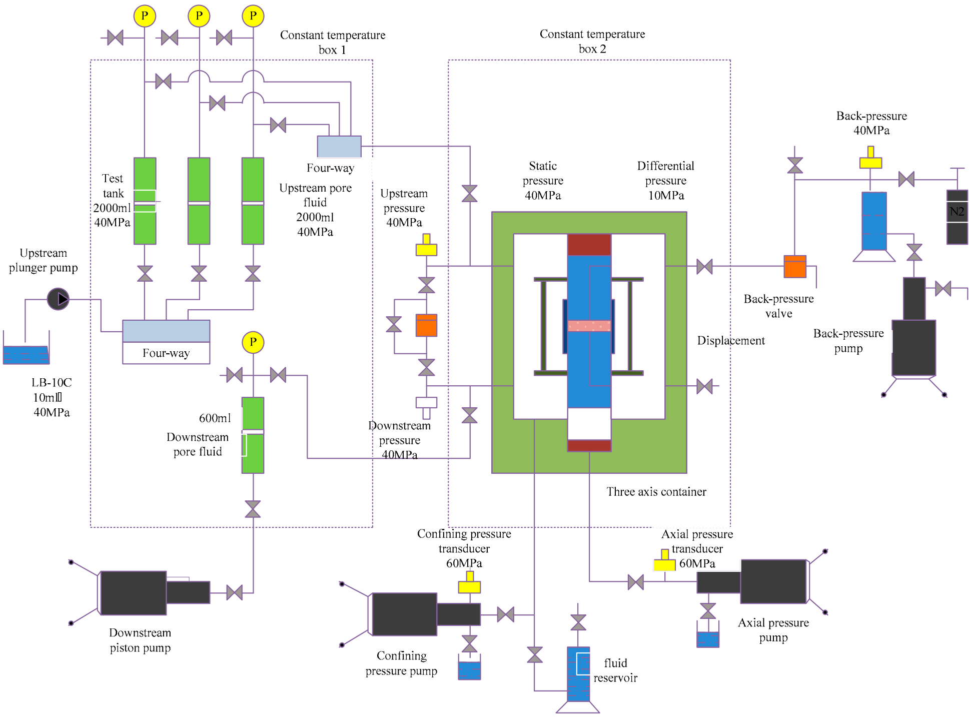

Figure 1. Experimental setup of HKY-3 pressure transmission device.

2.2.6. Low Temperature Nitrogen Adsorption Test

The Longtan coal and the Longmaxi shale samples were crushed and sieved between 60 to 80 meshes. Each 5 g sample was immersed in 1# compound surfactants and 0.8% MMH-2 solutions for 24 h. Then the samples were dried at 100 °C for 2 h. Before the test, all of the samples were outgassed under vacuum at 110 °C for 10 h. The low temperature nitrogen adsorption experiment was performed by a Micromeritics ASAP 2020 surface area and porosity analyzer (Micromeritics, Norcross, GA, USA) at −195.79 °C (liquid nitrogen temperature).

2.2.7. Performance Evaluation of Water-Based Drilling Fluid

(1) Basic performances

An optimized formulation of water-based drilling fluid (WBDF) is shown in Table 3. The order of additives was as follows: after adding bentonite to the water, a sixteen-hour hydration procedure was induced, and then the additives were poured into the mud in order of fluid loss additive 1, fluid loss additive 2, and shale inhibitor. For the water-based drilling fluid proposed in this paper, the 1# compound surfactants (0.001 wt% CS-4 + 0.001 wt% CS-1 + 0.001 wt% CS-3) and the organic MMH-2 needed to be added before the bentonite to prevent inhomogeneous dispersion. The remaining steps were the same.

Table 3. Composition of the water-based drilling fluid.

Additive Type	Additive Name	Concentration (wt%)	Lab Unit (per 360 cm^3)	Field Unit (per bbl)
base fluid	fresh water	87.5	315 cm^3	0.88 bbl
clay	sodium bentonite	4	14.4 g	14.4 lbm
fluid loss additive 1	sodium carboxymethyl cellulose	1.5	5.4 g	5.4 lbm
fluid loss additive 2	lignite resin	2	7.2 g	7.2 lbm
shale inhibitor	potassium chloride	5	18 g	18 lbm

Basic performances including rheological properties, American Petroleum Institute (API) fluid loss, and pH, were measured based on the newest API 13RD standards. The rheological properties were measured with a ZNN-D6 six-speed rotary viscometer. The readings at 600 and 300 rpm were marked as θ_{600} and θ_{300}. The apparent viscosity (AV, cP), plastic viscosity (PV, cP), and yield point (YP, lbf/100 sq ft) of the WBDF were calculated, respectively, according to Equations (2)–(4):

$$AV = 0.5 \times \theta_{600} \tag{2}$$

$$PV = \theta_{600} - \theta_{300} \tag{3}$$

$$YP = \theta_{300} - PV \tag{4}$$

The API fluid loss (FL) of the WBDF was measured with a ZNS-5A moderate pressure filter press at 0.69 MPa (100 psi) at ambient temperature for 30 min. Furthermore, the pH was measured with PHS-3C pH meter.

(2) Inhibition capability

Rolling recovery rate and linear swelling rate were used to evaluate the inhibition capability of drilling fluids to shale or coal samples. Fifty grams of 4 to 10-mesh coal or shale samples (simulated cuttings) were added into three different aging cans, which contained three different drilling fluids (WBDF, WBDF + 3 wt %MMH-1, and WBDF + 0.8 wt% MMH-2). The rolling test was run at 80 °C for 16 h. The cuttings were recovered by a 40-mesh sieve. The recovered cuttings were dried in a hot-roll oven at 100 °C for 4 h and weighed after being cooled under ambient temperature. The rolling recovery rate was calculated according to Equation (5):

$$R = \mathrm{m}/50 \tag{5}$$

where m is the weight (g) of the samples after being rolled at 80 °C for 16 h. The higher the shale or coal samples recovery rate was, the better the inhibition performance of the test liquid.

Linear swelling tests were carried out using a ZNP-1 expansion tester. Artificial coal cores were made of 1 mL of sodium silicate, 1 mL of calcium chloride, and 5 g of 80-mesh coal powders. The mixture was suppressed for 15 min under 20 MPa. Then the cores were put into the slot of the expansion tester, where time-dependent swelling increment was measured every 30 min for 8 h.

(3) Formation damage test

Reduction of reservoir permeability can be caused by invasion of solid particles and filtrate in a drilling fluid, which has a negative impact on CMG production at a later stage. Gas permeability of coal samples before and after contamination of various drilling fluids was tested by a JHGP gas permeability tester.

(4) Anti-pollution test

To evaluate pollutants (inorganic salts, drilling cuttings, etc) resistance properties of drilling fluids, a series of anti-pollution tests were carried out. Three wt% NaCl, 1 wt% $CaCl_2$, and 5 wt% attapulgite (simulated drilling cuttings) were used to simulate the possible pollutants in the drilling process of coal measure strata.

(5) Biotoxicity test

Biotoxicity of drilling fluid was determined by the photobacteria method [45]. Luminous intensity of luminescent bacteria is closely related to the toxicity of drilling fluid. Prepared drilling fluids were mixed with 3% NaCl in a ratio of 1 to 9. Then the mixtures' luminosity were tested by a biotoxicity tester after standing for 60 min. Results were compared to the luminosity of 3 wt% NaCl. Then the LC_{50} of drilling fluids were determined when the relative luminosity was decreased by 50%. Furthermore, the toxicity of drilling fluids was assessed following the classification criteria of API shrimp biotoxicity [45].

3. Results and Discussion

3.1. Surface Electrical Property Analysis

Figure 2 shows surface potential variations of the Longtan coal samples with the water solution shifting from acidic to alkaline, which were consistent with the results of Wang et al. [46], which were that the coal fines were usually negatively charged in water system The Longtan coal samples had positive charges under acidic conditions and negative charges under alkaline conditions with an isoelectric point of about 7. The result was consistent with Maršálek et al. [47], where the zeta potential of activated coal fines decreased with the increasing pH of water. That was due to the abundance of free hydroxyl ions in water under acid conditions, which were easy to combine with the coal surface [41].

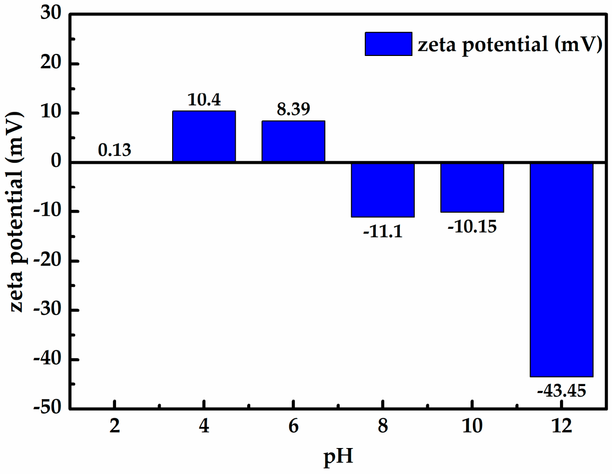

Figure 2. Relationship between zeta potential of the Longtan coal surface and pH.

Drilling fluid is usually weakly alkaline. According to Figure 2, the coal surface is usually negatively charged during the drilling process, which can lead to wellbore instability. Here, the higher the absolute value of the zeta potential, the more stable the drilling fluid is.

As shown in Table 4, with the addition of cationic surfactant CS-5 and organic MMH-2, the zeta potential of the Longtan coal was reversed from negative to positive. Due to the positive hydrophilic group of the cationic surfactant and the positive charge of MMH, these additives were easy to combine with the negative groups on the coal surface, and thus could effectively inhibit coal fines dispersion, and increase the stability of the wellbore.

Table 4. Effect of different dispersions on the surface zeta potential of coal.

Dispersions	Zeta Potential (mV)
fresh water	−3.63
fresh water + 3%MMH-1	−21.75
fresh water + 0.8%MMH-2	19.75
fresh water + 0.2%AS-1	−54.05
fresh water + 0.2%CS-5	47.25

As shown in Table 5, with the addition of MMH additives (MMH-1 and MMH-2), the zeta potential of the WBDF was increased from −56.80 mV to −30.4 mV and −31.8 mV, respectively, while the conventional drilling fluid’s zeta potential was −45 mV [41].

Table 5. Effect of different types of MMH on the zeta potential of filtrate.

Formula	Zeta Potential (mV)
WBDF	−56.80
WBDF + 3%MMH-1	−30.40
WBDF + 0.8%MMH-2	−31.80

Due to electrostatic force, MMH can combine with bentonite. Not only can this reaction reduce the negative charge of drilling fluid, but it can also make the drilling fluid has a "solid–liquid" duality, where under static conditions the MMH drilling fluid appears to be in a solid state with a certain elasticity, while under a dynamic situation (stirring) it shows great shear-thinning properties and good flowability [48], which is beneficial to wellbore stability.

3.2. Effect of Surfactants on Wettability of Rock Samples

As shown in Figure 3, the surface tension of water was reduced sharply by a 0.01–0.1 wt% concentration of surfactant. The curve tended to be steady thereafter. It is presumed that critical micelle concentration (CMC concentration) of these surfactants was around 0.01–0.1 wt%. Determination of CMC concentration is critical for the optimization of surfactant concentration. When the concentration is too high, the surfactant molecules will be aggregated to form micelles, which makes it difficult for the molecules to adsorb on the rock surface.

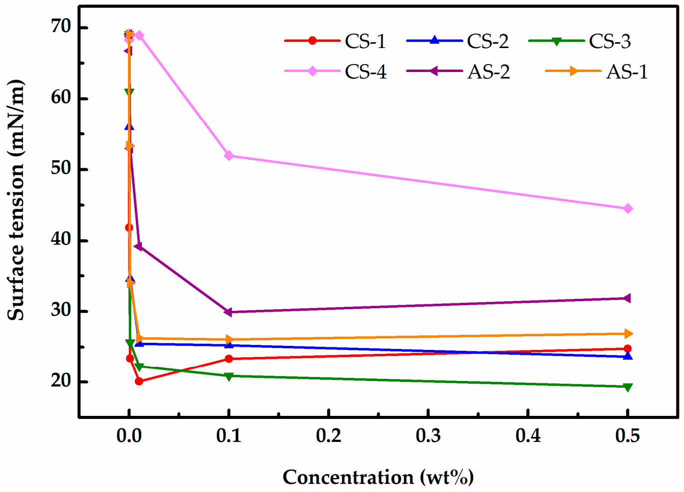

Figure 3. Relationship between surface tension vs surfactant concentration.

Figures 4 and 5 show the effects of different types of surfactants on contact angles of the Longmaxi shale and the Longtan coal samples.

As shown in Figure 4, after being treated with anionic surfactants (AS-1 and AS-2), the surface of the Longmaxi shale remained hydrophilic and all of the contact angles were below 60°, whereas the contact angles of the Longtan coal samples increased. Relatively, Figure 5a reveals that after being treated with cationic surfactants, the hydrophilicity of the Longmaxi shale was decreased, and after being treated with CS-3, the contact angle of the Longmaxi shale reached 98.5°. As for the Longtan coal (Figure 5b), the cationic surfactant CS-3 also increased the contact angle to a certain extent, but CS-4 seemed to be the most effective.

There are two mechanisms to describe the interaction of surfactants and rock samples: chemical adsorption and physical adsorption [49–51]. Taking the Longtan coal samples as an example, XRD results showed a large amorphous content (Table 2), and the contact angle results revealed that the Longtan coal samples were weakly hydrophilic (Figure 5), which indicated a large number of benzene rings and cycloalkyl groups attached to aromatic structures on the coal surface.

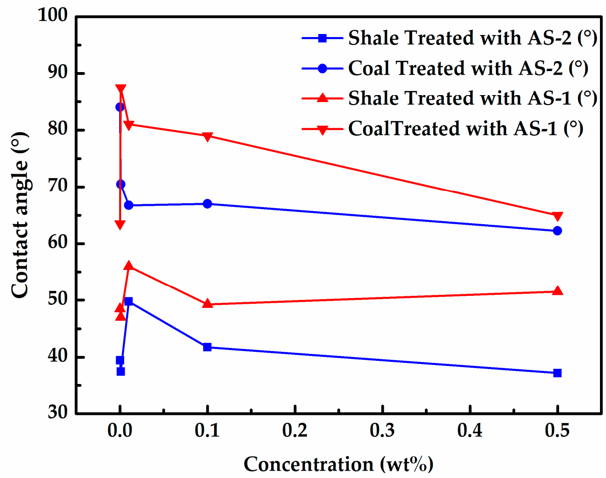

Figure 4. Effect of anionic surfactants to the contact angles of the Longmaxi shale and the Longtan coal samples.

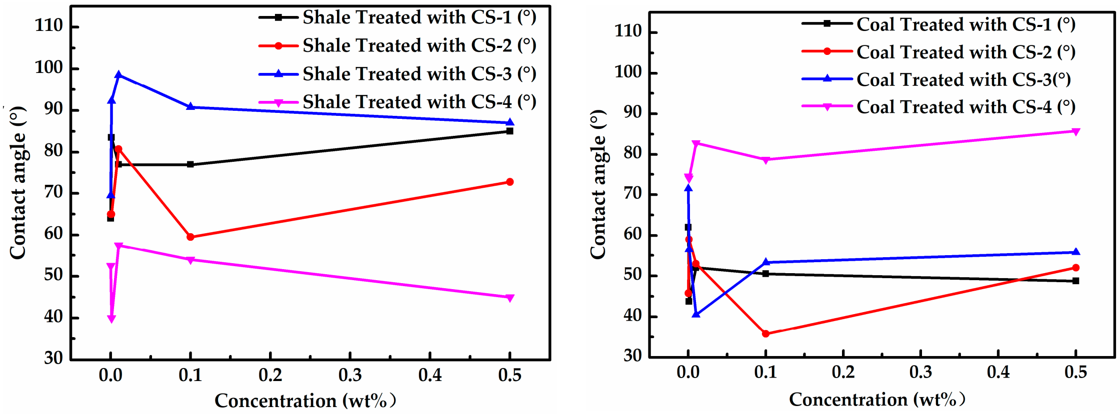

(**a**) (**b**)

Figure 5. Effect of cationic surfactants to the contact angles of the (**a**) Longmaxi shale and (**b**) the Longtan coal samples.

As shown in Figure 4, the contact angle of coal treated with AS-1 was relatively higher than that of AS-2, probably because AS-1 molecules were easier to adsorb on the coal surface because of the benzene rings. In contact with cationic surfactants (Figure 5b), the contact angle of the Longtan coal samples reduced sharply except CS-4, and the zeta potential increased, which indicated the existence of an electrostatic mechanism (physical adsorption). Alkyl chains of the cationic surfactants were united to the Longtan coal surface, and the polar end of the surfactant pointed to the water, thus making the Longtan coal surfaces more hydrophilic. Among these cationic surfactants, only CS-4 contained benzene rings, the Alkyl chains of the CS-4 were united to the Longtan coal surface, and the benzene rings pointed to the water, forming a hydrophobic film. Therefore the contact angle of the Longtan coal after treatment with CS-4 was higher.

As for the Longmaxi shale samples, due to the large amount of clay mineral content (Table 1), it can be concluded that electrostatic and hydrogen bonding played an important role in the adsorption process [8]. The hydrophilic polar end of the surfactant was attached to the surface of the Longmaxi shale by electrostatic forces and hydrogen bonds. The hydrophobic end of the surfactant pointed to the water, forming a hydrophobic film [51,52]. As surfactant concentration increased and exceeded the CMC concentration (0.01–0.1 wt%), the molecules gradually aggregated to form micelles, and the arrangement on the surface of the Longmaxi shale gradually became disordered, and thus the hydrophobicity was reduced.

As shown in Figures 4 and 5, both the Longtan coal and the Longmaxi shale surfaces were hydrophilic. To reduce the capillary force in the CMG reservoir, the contact angles of the Longmaxi shale and the Longtan coal must ideally remain around 90° simultaneously. According to previous results (Figure 4 to Figure 5), it is difficult to balance the wettability between the Longmaxi shale and the Longtan coal samples using only one kind of surfactant. A set of compound surfactants was optimized via an orthogonal experiment, as listed in Table 6.

Table 6. Experiment design of compound surfactants via orthogonal methods.

Compound Surfactants Combination	CS-3 (%)	CS-1 (%)	CS-4 (%)
1#	0.001	0.001	0.001
2#	0.001	0.005	0.005
3#	0.001	0.01	0.01
4#	0.005	0.001	0.005
5#	0.005	0.005	0.01
6#	0.005	0.01	0.001
7#	0.01	0.001	0.01
8#	0.01	0.005	0.001
9#	0.01	0.01	0.005

Figure 6 shows the effect of compound surfactants on the surface tension and contact angles of the Longmaxi shale and the Longtan coal samples. With the addition of the compound surfactants, the surface tension was clearly reduced from 69.08 mN/m (water surface tension) to less than 30 mN/m. After being treated with the 1# compound surfactant combination (0.001 wt% CS-4 + 0.001 wt% CS-1 + 0.001 wt% CS-3), the contact angles of the Longmaxi shale and the Longtan coal were 89° and 86°, respectively, which indicated that both the Longtan coal and the Longmaxi shale surfaces started to appear weakly hydrophilic. Due to the low concentration (meaning they are quite cost effective) of each surfactant and great wettability adjustment ability, the optimized compound surfactant formula was 0.001 wt% CS-4 + 0.001 wt% CS-1 + 0.001 wt% CS-3.

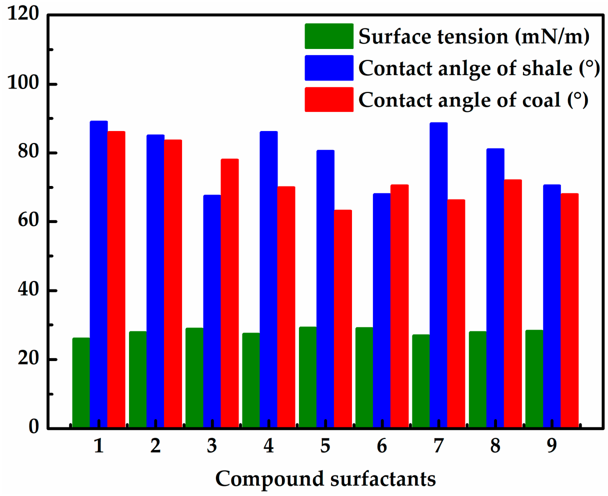

Figure 6. Effect of the optimized compound surfactants on surface tension and contact angle of shale or coal samples.

FT-IR spectroscopy measurements on the Longmaxi shale and the Longtan coal samples were conducted to better illustrate the adsorption mechanism of surfactants (Figure 7). Compared to raw coal (Figure 7a), there was no new adsorption peak after treatment with compound surfactants, indicating that physical adsorption was the dominant factor. As shown in Figure 7b, after being treated with compound surfactants, there was a new absorption peak at 3610.66 cm^{-1}, which was linked to

OH-stretching of structural hydroxyls. It can be speculated that the adsorption mechanism of these compound surfactants is chemical adsorption via hydrogen bonds along with physical adsorption.

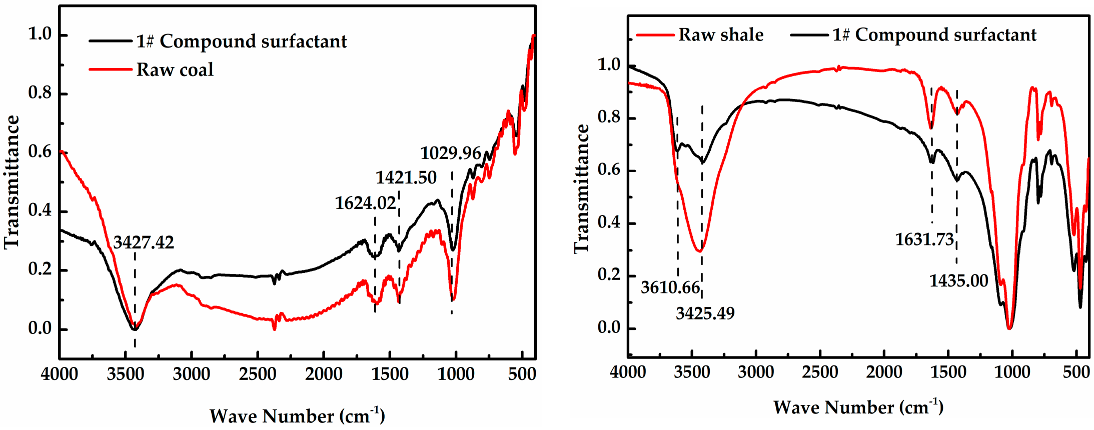

(**a**) (**b**)

Figure 7. FT-IR spectrum of the Longtan coal (**a**) and the longmaxi shale (**b**) samples before an after treatment with compound surfactants.

As shown in Table 7, with the addition of the 1# compound surfactant combination, the contact angle of the Longmaxi shale increased from 33.5° to 45.5°, while the contact angle of conventional drilling fluid is only 34.5° [51]. Similarly, the contact angle of coal was up to 65°, an increase of 18° compared to the WBDF, while the contact angle of the conventional drilling fluid was 52° [53]. Hydrophilic properties of the Longmaxi shale and the Longtan coal were weakened. However, due to the complex formulation of WBDF, the contact angle of the Longmaxi shale and the Longtan coal were not as high as in the fresh water the presence of the 1# compound surfactant. The stability of the surfactant needs to be improved in future studies.

Table 7. Effect of optimized compound surfactants on contact angle (°) of the Longmaxi shale and the Longtan coal.

Formula	Contact Angle of the Longmaxi Shale (°)	Contact Angle of the Longtan Coal (°)
WBDF	33.5	47
WBDF + 3wt% MMH − 1 + 1# compound surfactants	45.5	65

3.3. Pressure Transmission Test

The primary factor of wellbore instability in shale formations is transmission of hydrostatic pressure of drilling fluid and infiltration of filtrate into wellbores [54]. As shown in Figure 8, pressure transmission test results showed the remarkable effects of the compound surfactants and MMH in retarding pore pressure transmission on the Longtan coal and the Longmaxi shale.

As shown in Figure 8a, when water was used as a medium, the Longmaxi shale started to crack at about 10 h and was broken at about 30 h. When compound surfactant solution was used as the medium, the Longmaxi shale were intact, and the calculated permeability dropped sharply from 2.15×10^{-3} mD to 2.79×10^{-6} mD. When the MMH-1 solution was used as the medium, the calculated permeability was 8.78×10^{-7} mD.

Similarly, when the upstream pressure was 2 MPa and water was used as a medium, the Longtan coal began to crack at about 0.5 h. When the compound surfactant solution was used as the medium, the Longtan coal sample remained intact, and the calculated permeability decreased sharply from 0.61 mD to 6.87×10^{-6} mD, while when MMH-1 was used as the medium, the permeability dropped to 2.134×10^{-4} mD.

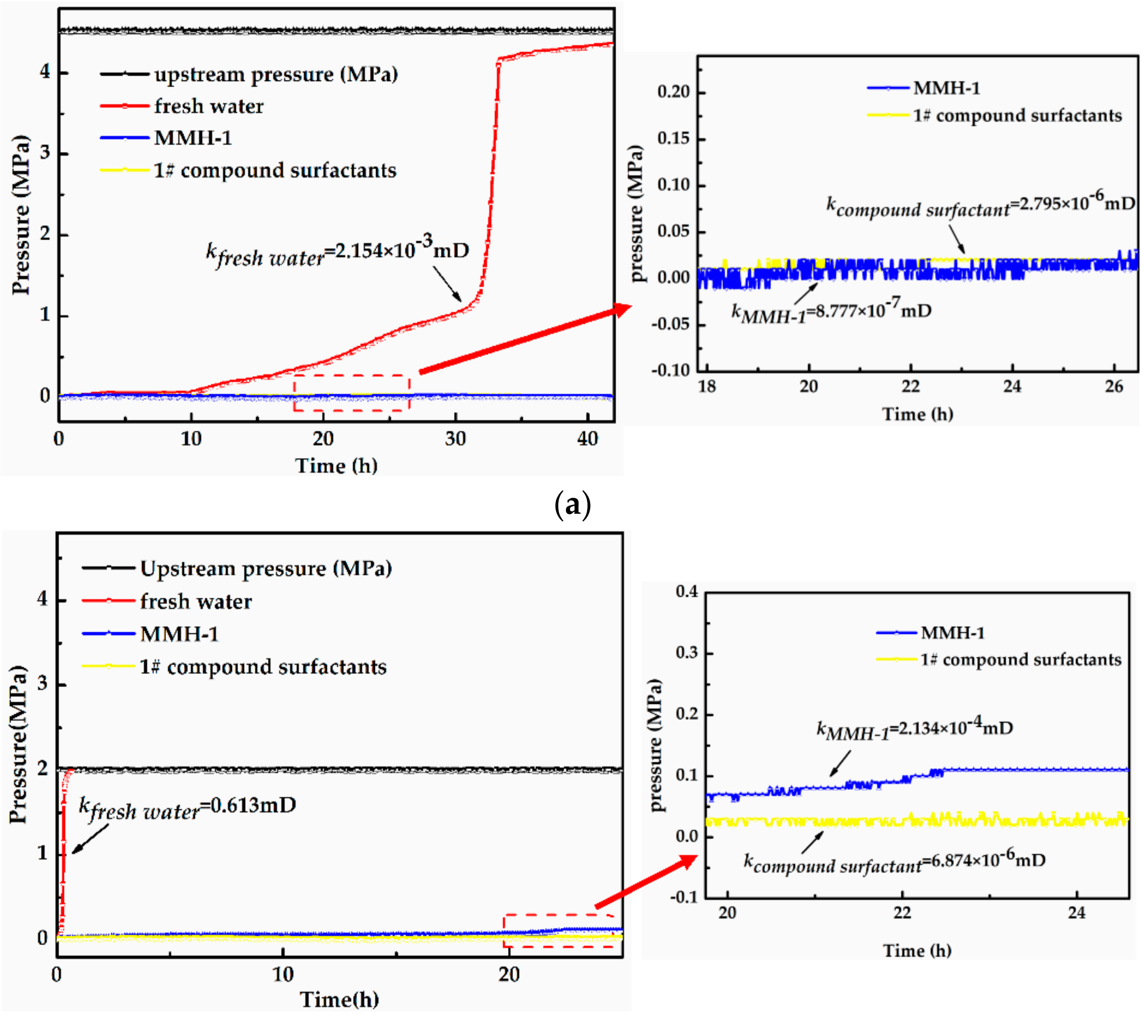

(**a**)

(**b**)

Figure 8. Effect of MMH-1 and 1# compound surfactants (0.001 wt% CS-4 + 0.001 wt% CS-1 + 0.001 wt% CS-3) on retarding pressure transmission of shale and coal. (**a**) Shale sample pressure curve versus time; (**b**) Coal sample pressure curve versus time.

3.4. Pore Structure Comparison Before and After Treatment with 1# Compound Surfactants and MMH-2

FT-IR results (Figure 7) revealed the adsorption mechanisms of different surfactants, and the adsorbed surfactants on the pore structure could not be ignored. A set of low temperature nitrogen adsorption tests were carried out to better understand the adsorption position of surfactants and MMH-2. As shown in Figure 9a, after being treated with 1# compound surfactants, pore volume (diameter larger than 100 nm) decreased significantly compared to the original shale sample, suggesting the adsorption site might have concentrated on the large pore throats. Furthermore, an increase of pore volume (diameter 70–90) was detected, although the reason remains unknown. Possibly, because the surfactant aggregated in large pore throats [55], the space between the surfactant micelles was mistaken for a shale pore. As for coal (Figure 9b), both MMH-2 and 1# compound surfactant minimized the pore volume effectively.

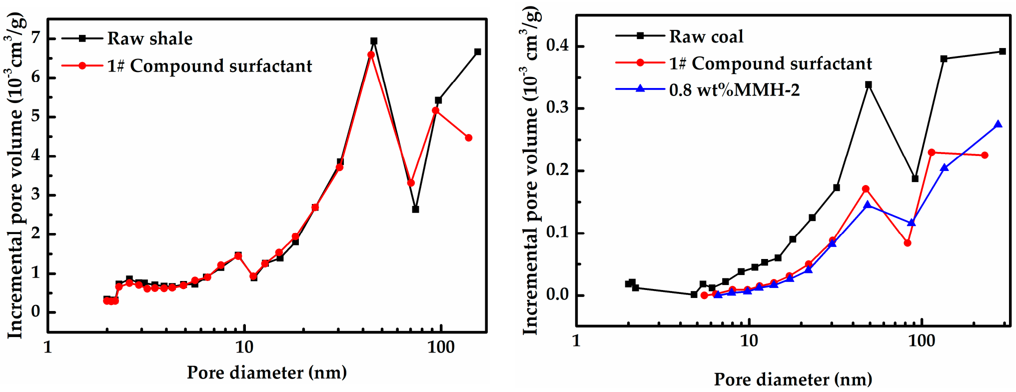

(**a**) (**b**)

Figure 9. Effect of 0.8 wt%MMH-2 and 1#compound surfactants (0.001 wt% CS-4 + 0.001 wt% CS-1 + 0.001 wt% CS-3) on decreasing pore volume of the Longmaxi shale (**a**) and the Longtan coal (**b**).

3.5. Water-Based Drilling Fluid Performance Test

According to the basic performance tests results shown in Table 8, apparent viscosity of the MMH-1 drilling fluid (WBDF + 3 wt% MMH-1 + 0.001 wt%CS-4 + 0.001 wt% CS-1 + 0.001 wt% CS-3) was slightly lower than that of the MMH-2 drilling fluid (WBDF + 0.8 wt% MMH-2 + 0.001 wt% CS-4 + 0.001 wt% CS-1 + 0.001 wt% CS-3), but its API filter loss was only 3.5 mL, which was much lower than that of the MMH-2 drilling fluid. Thus, the comprehensive performance of the MMH-1 drilling fluid was relatively better.

Table 8. Basic properties of the proposed drilling fluid formula.

Formula	μ_a (cP)	μ_p (cP)	τ_0 (lbf/100 sq ft)	FL$_{API}$ (mL)	pH	Lubrication Factor
WBDF+3wt%MMH-1+1# compound surfactants	33.5	21	23.94	7	10.39	0.18
WBDF+0.8wt%MMH-2+1# compound surfactants	38.5	22	31.6	10.5	8.38	0.17

Note: The lubrication factor of WBDF is 0.46; 1# compound surfactants are 0.001 wt% CS-4 + 0.001 wt% CS-1 + 0.001 wt% CS-3. μ_a is apparent viscosity, μ_p is plastic viscosity, τ_0 is yield point, FL$_{API}$ is American Petroleum Institute fluid loss.

As for the inhibition performance, the MMH-1 drilling fluid achieved a slightly higher rolling recovery rate (Figure 10) and a lower linear expansion rate (Figure 11) compared to the MMH-2 drilling fluid. Overall, the MMH-1 drilling fluid performed better and was more suitable for drilling in coal measure strata.

To better illustrate practicability potential of drilling fluids, formation damage characteristics (Table 9), anti-pollution ability (Table 10), and environmental protection ability of MMH-1 drilling fluid were evaluated. As shown in Table 9, the MMH-1 drilling fluid had a permeability damage rate of only 10% to the coal reservoir, and it could reduce the permeability reduction rate by 3.6% compared to the WBDF.

Table 10 shows the anti-pollution performance of the optimized drilling fluid (WBDF + 3 wt% MMH-1 + 1# compound surfactants). With the addition of inorganic salts and simulated drill cuttings (attapulgite), the viscosity (apparent viscosity, plastic viscosity) and yield point of these drilling fluids showed a slight decrease, which could be attributed to the flocculation of the bentonites [56,57]. The fluid loss appeared to increase when 5 wt% attapulgite was added. However, these changes of the MMH-1 drilling fluid varied within an acceptable range. It showed an excellent capability to withstand common pollutants that may appear in the drilling process of coal measure strata. Another key factor that affects drilling fluids properties is high temperature and high pressure, which need to be studied in the future.

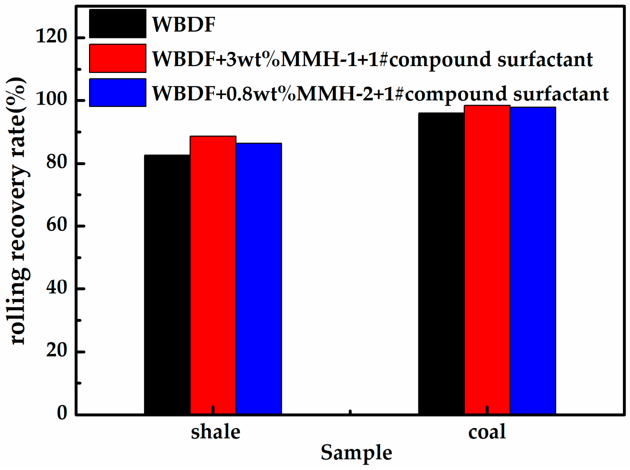

Figure 10. Effect of different drilling fluids on rolling recovery rates of the Longmaxi shale and the Longtan coal. Note: The formula of 1# compound surfactant is 0.001 wt% CS-4 + 0.001 wt% CS-1 + 0.001 wt% CS-3. The same as follows.

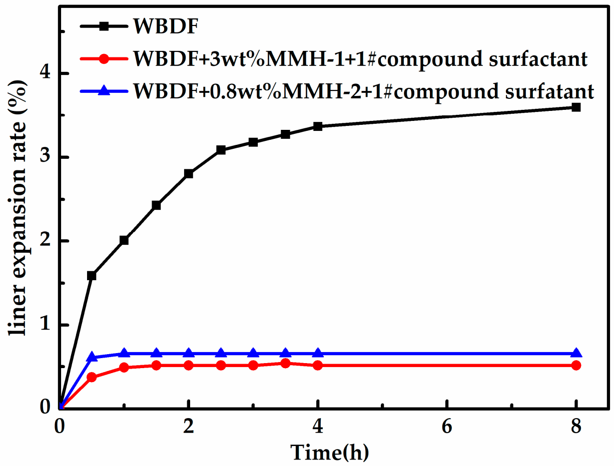

Figure 11. Effect of various drilling fluid on liner expansion rate of the Longtan coal.

Table 9. Effect of drilling fluid on coal sample's permeability.

Formula	k_0 (mD)	k_1 (mD)	Permeability Reduction Rate (%)
WBDF	1.25	1.08	13.6
WBDF + 3 wt% MMH-1 + 1#compound surfactants	0.60	0.54	10

Table 10. Anti-pollution test results.

Formula	μ_a (cP)	μ_p (cP)	τ_0 (lbf/100 sq ft)	FL_{API} (mL)
WBDF + 3 wt% MMH-1 + 1# compound surfactants	33.50	21.00	23.94	7.0
WBDF + 3 wt% MMH-1 + 1# compound surfactants + 3wt %NaCl	26.50	21.00	11.50	6.0
WBDF + 3 wt% MMH-1 + 1# compound surfactant + 1wt% $CaCl_2$	28.00	21.00	13.40	6.0
WBDF + 3 wt% MMH-1 + 1# compound surfactants + 5 wt% attapulgite	31.00	22.00	17.24	9.5

Note: 1# compound surfactants are 0.001 wt% CS-4 + 0.001 wt% CS-1 + 0.001 wt% CS-3. μ_a is apparent viscosity, μ_p is plastic viscosity, τ_0 is yield point, FL_{API} is American Petroleum Institute fluid loss.

3.6. Biotoxicity Evaluation

The LC_{50} (half-life lethal concentration of 96 h luminescent bacteria) of the MMH-1 drilling fluid is 294,000 ppm, as seen in Table 11, and it satisfies the emission standard (30,000 ppm), indicating that it has very low toxicity and is environmentally friendly.

Table 11. Biological toxicity level classification standard.

Level	Poisonous	High Toxicity	Moderate Toxicity	Slight Toxicity	Actually Non-Toxic	Emission Standard
LC_{50} (ppm)	<1	$1\sim10^2$	$10^2\sim10^3$	$10^3\sim10^4$	$>10^4$	$>3\times10^4$

3.7. Potential for Field Application

Water-based high inhibitive and low formation damage drilling fluids containing mixed metal hydroxide (MMH) and compound surfactants have been proposed for the first time. Due to its high inhibitive and low formation damage characteristics, this drilling fluid system can not only be used in coal measure strata, but also in single shale and coal formations. While in single coal formations, some additives, such as shale inhibitor (potassium chloride) and fluid loss additive 1 (sodium carboxymethyl cellulose), are not necessary. Furthermore, the proposed 1# compound surfactants showed great performance to increase the contact angle of the Longtan coal and the Longmaxi shale, decreasing their hydrophilicity, which could also be used in fracturing fluid to minimize water-blockage damage and protect the reservoir.

According to Table 10, the proposed drilling fluid system showed great tolerance to $CaCl_2$ and NaCl, indicating the stability when encountering formation water, while the viscosity and filtrate volume showed an increase after attapulgite (simulating drilling cuts) was added. Therefore, a set of four-stage solid control equipment (shale shaker, desander, desilter, centrifuge) was suggested during the drilling process.

4. Conclusions

A systematic study was carried out to characterize the wettability alteration ability and zeta potential adjustment to shale and coal of different types of surfactants and MMH. Based on the results, the following conclusions can be drawn:

(1) When the zeta potential was measured as a function of pH, the results show that the zeta potential of the Longtan coal decreases with increasing pH, the isoelectric point of the Longtan coal is around 7, and the cationic surfactant CS-5 could increase the zeta potential of the Longtan coal up to + 41.25 mV.

(2) According to the contact angle results, a cationic surfactant CS-3 could effectively increase the contact angle of shale up to 98.5°. Furthermore, a set of cationic compound surfactants (0.001 wt% CS-4 + 0.001 wt% CS-1 + 0.001 wt% CS-3) was optimized, which could increase the contact angle of the Longmaxi shale and the Longtan coal up 89° and 86°, respectively.

(3) The dominant adsorption mechanism between the cationic surfactant and the Longmaxi shale is via hydrogen bonds, while that of the Longtan coal was physical adsorption (via electrostatic forces).

(4) Pressure transmission test results show that MMH and the 1# optimized compound surfactants can effectively retard the transmission of pore fluid pressure and decrease the permeability of the core samples, thus increasing wellbore stability.

(5) A set of environmentally friendly water-based drilling fluid systems was proposed (4 wt% sodium bentonite +1.5 wt% sodium carboxymethyl cellulose +2 wt% lignite resin +5 wt% potassium chloride +3 wt% MMH-1 + 0.001 wt% CS-4 + 0.001 wt% CS-1 + 0.001 wt% CS-3). Based on the liner expansion results, the proposed drilling fluid system showed a great inhibitive property. Furthermore, the permeability results confirm its low-damage characteristic to CMG reservoirs.

Author Contributions: S.C. prepared the initial manuscript; Y.S. helped to complete the pressure transmission test of the Longtan coal; X.Y. helped to complete with the pressure transmission test of the Longmaxi shale; K.X. helped with the contact angle test of the Longtan coal; J.C. were responsible for the academic ideas.

Funding: The study is supported by the National Science Foundation of China (No. 41072111), the Key Project of Natural Science Foundation of Hubei Province (No. 2015CFA135), the Technical Innovation Special Project of Hubei Province (No. 2017AHB052), the Youth Chenguang Project of Science and Technology of Wuhan City (No. 2017050304010317) and the National Key Research and Development Program of China (No. 2018YFC1801705).

Acknowledgments: The authors would like to thank Hongbing Zhan at Texas A&M University for kind help in the revision of this article.

Conflicts of Interest: The authors declare no conflict of interest.

References

1. Shao, L.Y.; Yang, Z.Y.; Shang, X.X.; Xiao, Z.H.; Wang, S.; Zhang, W.L.; Lu, J. Lithofacies palaeogeography of the Carboniferous and Permian in the Qinshui Basin, Shanxi Province, China. *J. Palaeogeogr.* **2015**, *4*, 384–412. [CrossRef]
2. Yi, T.S.; Gao, W. Reservoir formation characteristics as well as co-exploration and co-mining orientation of Upper Permian coal-bearing gas in Liupanshui Coalfield. *J. China Coal Soc.* **2018**, *43*, 1553–1564. [CrossRef]
3. Fu, X.; Ge, Y.; Liang, W.; Li, S. Pressure control and fluid effect of progressive drainage of multiple superposed cbm systems. *Nat. Gas Ind.* **2013**, *33*, 35–39. [CrossRef]
4. Qin, Y.; Wu, J.G.; Shen, J.; Yang, Z.B.; Shen, Y.L.; Zhang, B. Frontier research of geological technology for coal measure gas joint-mining. *J. China Coal Soc.* **2018**, *43*, 1504–1516. [CrossRef]
5. Estes, B. Technology Focus: Drilling and completion fluids (November 2009). *J. Pet. Technol.* **2011**, *61*, 62. [CrossRef]
6. Gentzis, T.; Deisman, N.; Chalaturnyk, R.J. Effect of drilling fluids on coal permeability: Impact on horizontal wellbore stability. *Int. J. Coal Geol.* **2009**, *78*, 177–191. [CrossRef]
7. Cai, J.H.; Gu, S.; Wang, F.; Yang, X.Y.; Yue, Y.; Wu, X.M.; Chixotkin, V.F. Decreasing Coalbed Methane Formation Damage Using Microfoamed Drilling Fluid Stabilized by Silica Nanoparticles. *J. Nanomater.* **2016**, 1–11. [CrossRef]
8. Huang, W.; Li, X.; Qiu, Z.; Jia, J.; Wang, Y.; Li, X. Inhibiting the surface hydration of shale formation using preferred surfactant compound of polymine and tweleve alkyl two hydroxyethyl amine oxide for drilling. *J. Pet. Sci. Eng.* **2017**, *41*, 37–41. [CrossRef]
9. Yue, Q.S.; Chen, J.; Zou, L.P.; Jiang, G.Z.; Tian, Z.L.; Yang, H.L. Research on coalbed methane drilling fluid for horizontal well based on coal reservoir protection in qinshui basin. *J. China Coal Soc.* **2012**, *37*, 416–419. [CrossRef]
10. Yue, Q.S.; Ma, X.; Chen, J.; Jiang, G.Z. Instability mechanism of borehole and drilling fluid technical countermeasures for coalbed methane horizontal well in qinshui basin. *J. Yangtze Univ.* **2014**, *11*, 73–76. [CrossRef]
11. Zheng, L.H.; Su, G.D.; Li, Z.H.; Peng, R.; Wang, L.; Wei, P.F.; Han, S.X. The wellbore instability control mechanism of fuzzy ball drilling fluids for coal bed methane wells via bonding formation. *J. Nat. Gas Sci. Eng.* **2018**, *56*, 107–120. [CrossRef]
12. Vryzas, Z.; Kelessidis, V.C. Nano-based drilling fluids: A review. *Energies* **2017**, *10*, 540. [CrossRef]
13. Li, M.C.; Wu, Q.L.; Song, K.L.; De Hoop, C.F.; Lee, S.; Qing, Y.; Wu, Y.Q. Cellulose nanocrystals and polyanionic cellulose as additives in bentonite water-based drilling fluids: Rheological modeling and filtration mechanisms. *Ind. Eng. Chem. Res.* **2016**, *55*, 133–143. [CrossRef]
14. Ismail, A.R.; Aftab, A.; Ibupoto, Z.H.; Zolkifile, N. The novel approach for the enhancement of rheological properties of water-based drilling fluids by using multi-walled carbon nanotube, nanosilica and glass beads. *J. Pet. Sci. Eng.* **2016**, *139*, 264–275. [CrossRef]
15. Abdo, J.; Haneef, M.D. Clay nanoparticles modified drilling fluids for drilling of deep hydrocarbon wells. *Appl. Clay Sci.* **2013**, *86*, 76–82. [CrossRef]
16. Barry, M.M.; Jung, Y.; Lee, J.K.; Phuoc, T.X.; Chyu, M.K. Fluid filtration and rheological properties of nanoparticle additive and intercalated clay hybrid bentonite drilling fluids. *J. Pet. Sci. Eng.* **2015**, *127*, 338–346. [CrossRef]

17. Gerogiorgis, D.I.; Clark, C.; Vryzas, Z.; Kelessidis, V.C. Development and parameter estimation for a multivariate Herschel-Bulkley rheological model of a nanoparticle-based smart drilling fluid. In Proceedings of the 12th International Symposium on Process Systems Engineering and 25th European Symposium on Computer Aided Process Engineering, PT C 2015, Copenhagen, Denmark, 31 May–4 June 2015. [CrossRef]
18. Reilly, S.I.; Vryzas, Z.; Kelessidis, V.C.; Gerogiorgis, D.I. First-principle rheological modelling and parameter estimation for nanoparticle-based smart drilling fluids. In Proceedings of the 26th European Symposium on Computer Aided Process Engineering, PT A 2016, Portoroz, Slovenia, 12–15 June 2016. [CrossRef]
19. Zhang, X.; Sun, W.; Ren, D.; Liu, D.; Nan, J. Effects of surfactant on the electrical property of ultra-low permeability sandstone reservoir:the Upper Triassic Chang 8 formation in Longdong area of Ordos basin as an example. *Geol. Sci. Technol. Inf.* **2016**, *35*, 235–241.
20. Adibhatla, B.; Mohanty, K.K. Oil recovery from fractured carbonates by surfactant-aided gravity drainage: Laboratory experiments and mechanistic simulations. *SPE Res. Evaluation Eng.* **2006**, *11*, 119–130. [CrossRef]
21. Hirasaki, G.; Zhang, D.L. Surface chemistry of oil recovery from fractured, oil-wet, carbonate formations. *SPE J.* **2004**, *9*, 151–162. [CrossRef]
22. Young, T. An essay on the cohesion of fluids. *Philos. Trans. Royal Soc. Lond.* **1805**, *95*, 65–87. [CrossRef]
23. Förch, R.; Schönherr, H.; Jenkin, A.T.A. Surface Design: Applications in Bioscience and Nanotechnology. *Mater. Today* **2009**, *12*, 1–54. [CrossRef]
24. Hu, Y.L.; Wu, X.M. Research on coalbed methane reservior water blocking damage mechanism and anti-water blocing. *J. China Coal Soc.* **2014**, *39*, 1107–1111. [CrossRef]
25. Liang, L.; Xiong, J.; Liu, X. Effects of hydration swelling and wettability on propagation mechanism of shale formation crack. *Pet. Geol. Exp.* **2014**, *36*, 780–786. [CrossRef]
26. Alvarez, J.O.; Schechter, D.S. Wettability Alteration and Spontaneous Imbibition in Unconventional Liquid Reservoirs by Surfactant Additives. *SPE Res. Evaluation Eng.* **2017**, *20*, 107–117. [CrossRef]
27. Quintero, L. An Overview of Surfactant Applications in Drilling Fluids for the Petroleum Industry. *J. Dispers. Sci. Technol.* **2002**, *23*, 393–404. [CrossRef]
28. Yunita, P.; Irawan, S.; Kania, D. Optimization of water-based drilling fluid using non-ionic and anionic surfactant additives. *Procedia Eng.* **2016**, *148*, 1184–1190. [CrossRef]
29. Shadizadeh, S.R.; Moslemizadeh, A.; Dezaki, A.S. A novel nonionic surfactant for inhibiting shale hydration. *Appl. Clay Sci.* **2015**, *118*, 74–86. [CrossRef]
30. Cai, J.H.; Ye, Y.; Cao, W.J.; Yang, X.Y.; Wu, X.M. Experimental study on the effect of drilling fluid wettability on shale wellbore stability. *J. China Coal Soc.* **2016**, *41*, 228–233. [CrossRef]
31. Nasralla, R.A.; Nasr-El-Din, H.A. Double-Layer Expansion: Is It a Primary Mechanism of Improved Oil Recovery by Low-Salinity Waterflooding? *SPE Res. Evaluation Eng.* **2014**, *17*, 49–59. [CrossRef]
32. Zadaka, D.; Radian, A.; Mishael, Y.G. Applying zeta potential measurements to characterize the adsorption on montmorillonite of organic cations as monomers, micelles, or polymers. *J. Colloid Interface Sci.* **2010**, *352*, 171–177. [CrossRef]
33. Erbil, H.Y. *Surface Chemistry of Solid and Liquid Interfaces*; Blackwell Pub: Oxford, UK, 2006.
34. Su, C.M.; Fu, J.T. Research on the changing tendency of zeta potential of the clay minerals and drilling fluid. *Driuing Fluid Complet. Fluid* **2002**, *19*, 1–4. [CrossRef]
35. Zhang, C.G.; Hou, W.G. Electrical behavior, inhibition, wall stability and reservoir protection. *Drill. Fluid Complet. Fluid* **2002**, *19*, 5–8. [CrossRef]
36. Alkan, M.; Demirbaş, Ö.; Doğan, M. Electrokinetic properties of kaolinite in mono- and multivalent electrolyte solutions. *Microporous Mesoporous Mater.* **2005**, *83*, 51–59. [CrossRef]
37. Buckley, J.S.; Liu, Y.; Monsterleet, S. Mechanisms of wetting alteration by crude oils. *Spe J.* **1998**, *3*, 54–61. [CrossRef]
38. Alvarez, J.O.; Schechter, D.S. Application of wettability alteration in the exploitation of unconventional liquid resources. *Pet. Explor. Dev.* **2016**, *43*, 832–840. [CrossRef]
39. Arif, M.; Jones, F.; Barifcani, A.; Iglauer, S. Influence of surface chemistry on interfacial properties of low to high rank coal seams. *Fuel* **2017**, *194*, 211–221. [CrossRef]
40. Song, Y. Zeta Potential of the surface of fine coal. *J. Fuel Chem. Technol.* **1998**, *16*, 245–252.
41. Li, X.; Kang, Y.; Yin, Z. Surface electricity and wettability of coal rock under the condition of different chemical environments. *J. China Univ. Min. Technol.* **2014**, *43*, 864–869. [CrossRef]

42. Shu, Y.; Yan, J. Characterization and prevention of formation damage for fractured carbonate reservoir formations with low permeability. *Pet. Sci.* **2008**, *5*, 326–333. [CrossRef]
43. Han, H.; Zhong, N.; Jiao, S. Scanning electron microscope observation of pores in mud stone and shale. *J. Chin. Electron Microsc. Soc.* **2013**, *32*, 325–329. [CrossRef]
44. Yang, J.; Fu, Y.Q.; Chen, H.F.; Zeng, L.X.; Li, J.S. Rock mechanical characteristics of shale reservoirs. *Nat. Gas Ind.* **2012**, *32*, 12–14. [CrossRef]
45. Huang, X. Comparson of biological toxicity assessment methods for drilling fluids. *Environ. Prot. Oil Gas Fields* **2006**, *16*, 25–27. [CrossRef]
46. Wang, B.; Min, L.I.; Zhao, Q.; Qin, Y.; Xie, K. Relationship between surface potential and functional groups of coals. *J. Chem. Ind. Eng.* **2004**, *55*, 1329–1334. [CrossRef]
47. Maršálek, R. The Influence of Surfactants on the Zeta Potential of Coals. *Energy Sources Part A Recovery Util. Environ. Eff.* **2008**, *31*, 66–75. [CrossRef]
48. Su, C.M.; Liu, R.S.; Yu, P.Z.; Wang, C.P. Study and application of electropositive drilling fluid system. *Oil Drill. Prot. Technol.* **2004**, *26*, 17–21. [CrossRef]
49. Liu, S.; Liu, X.; Guo, Z.; Liu, Y.; Guo, J.; Zhang, S. Wettability modification and restraint of moisture re-adsorption of lignite using cationic gemini surfactant. *Colloids Surf. A Physicochem. Eng. Asp.* **2016**, *508*, 286–293. [CrossRef]
50. Chen, S.; Wang, S.; Li, L.; Qu, J.; Tao, X.; He, H. Exploration on the mechanism of enhancing low-rank coal flotation with cationic surfactant in the presence of oily collector. *Fuel* **2018**, *227*, 190–198. [CrossRef]
51. Yue, Y.; Chen, S.; Wang, Z.; Yang, X.; Peng, Y.; Cai, J. Improving wellbore stability of shale by adjusting its wettability. *J. Pet. Sci. Eng.* **2018**, *161*, 692–702. [CrossRef]
52. Zhou, L.; Das, S.; Ellis, B.R. Effect of surfactant adsorption on the wettability alteration of gas-bearing Shales. *Environ. Eng. Sci.* **2016**, *33*, 766–777. [CrossRef]
53. Shi, Y.P.; Chen, S.Y.; Yang, X.Y.; Yu, L. Enhancing wellbore stability of coal measure strata by electricla inhibition and wettability control. *J. Pet. Sci. Eng.* **2019**, *174*, 544–552. [CrossRef]
54. Van Oort, E.; Hale, A.; Mody, F.; Roy, S. Transport in shales and the design of improved water-based shale drilling fluids. *SPE Drill. Complet.* **1996**, *11*, 137–146. [CrossRef]
55. Liu, X.; Liu, S.; Fan, M.; Guo, J.; Li, B. Decrease in hydrophilicity and moisture readsorption of Manglai lignite using lauryl polyoxyethylene ether: Effects of the HLB and coverage on functional groups and pores. *Fuel Process. Technol.* **2018**, *174*, 33–40. [CrossRef]
56. Abdo, J.; Haneef, M.D. Nano-enhanced drilling fluids: Pioneering approach to overcome uncompromising drilling problems. *J. Energy Resour. Technol. Trans. ASME* **2012**, *134*, 014501. [CrossRef]
57. Vryzas, Z.; Kelessidis, V.C.; Nalbantian, L.; Zaspalis, V.; Gerogiorgis, D.I.; Wubulikasimu, Y. Effect of temperature on the rheological properties of neat aqueous Wyoming sodium bentonite dispersions. *Appl. Clay Sci.* **2017**, *136*, 26–36. [CrossRef]